Microgravity Opposed Flow Flame Spread in Polyvinyl Chloride Tubes

G.W. Sidebotham*
Department of Mechanical Engineering
The Cooper Union for the Advancement of Science and Art
51 Astor Place
New York, NY 10003

and

S.L. Olson
NASA Glenn Research Center
Cleveland, Ohio

Abstract
The effects of gravity on opposed flow flame spread along the inner surface of polyvinyl chloride (PVC) tubes against a flow of pure oxygen were investigated experimentally. In microgravity, the flame spread rate exhibited a 1.25 power law dependency between a low opposed flow velocity ignition limit of 1.4 cm/s and 6.3 cm/s, and an abrupt change in power law slope to approximately square root for opposed flow velocities between 6.3 cm/s and 15.4 cm/s. The effects of gravity were greater for horizontal flames compared with vertical flames. These results suggest that a ground-based flammability test can be designed based on this geometry for the purpose of screening materials for space flight.

Introduction

It is difficult to investigate low-flow quenching limits in opposed flow flame spread due to induced buoyant flow [1]. However, low flow quenching limits are known to exist because they have been measured for thermally thin samples in microgravity environments [2]. The present study reports on a terrestrially-based opposed flow flame spread geometry that exhibits a low-flow quenching limit. This geometry was discovered during the course of investigation of a unique fire safety problem during surgical procedures where it was shown that the accidental ignition of polyvinyl chloride (PVC) endotracheal tubes (breathing tubes used during general anesthesia) by high energy surgical devices results in an opposed flow flame that spreads along the inner surface of the tube [3, 4, 5].

The following simple, reproducible experiment can be used for the fundamental study of flame spread phenomena. An oxidizer flow is established through a flammable solid material in tube form, and an ignition source is applied to the free end, or through a perforation in the tubing (created by a laser, for example). A flame quickly establishes inside the tube and spreads toward the oxidizer source at a measurable velocity.

Specific Objectives

The primary goal of the present investigation is to describe the flame types and measure the opposed flow flame spread rate along the inner surface of PVC tubes in microgravity conditions. A secondary goal is to determine the extent of a buoyant regime by comparing the flame spread rates in normal and microgravity. The possibility of developing a terrestrial-based test for screening materials is considered.

Experimental

The tests were conducted in the 2.2 second drop tower at the NASA Glenn Research Center. A general purpose rig consisting of a 25.4 cm inner diameter, 50.4 cm inner height cylindrical chamber and instrumentation was used, similar to that described by Olson (1991). A schematic and photograph of the test apparatus is shown in Figure 1. The chamber was filled with nitrogen to the test pressure. The basic experiment consists of flowing oxygen (stored in a 75 cc cylinder on the rig) through a tube sample, igniting it with a hot wire in normal gravity, and dropping it after a flame is established (propagating toward the oxygen source) to observe microgravity effects. Two opposed flow flame orientations were studied: horizontal and vertical (downward spreading). All tests were conducted using 0.635 cm inner diameter, 0.953 cm outer diameter clear polyvinyl chloride (PVC) tubing

* Corresponding author: sidebo@cooper.edu
Proceedings of the 2006 Technical Meeting of the Central States Section of The Combustion Institute

manufactured by New Age Industries (product: 1101149—Clearflo). This plasticized PVC tubing was used as it provides direct visual observation of the flame, closely resembles the form and composition of endotracheal tubes used in surgery, and was used in previous normal gravity studies [3, 4, 5].

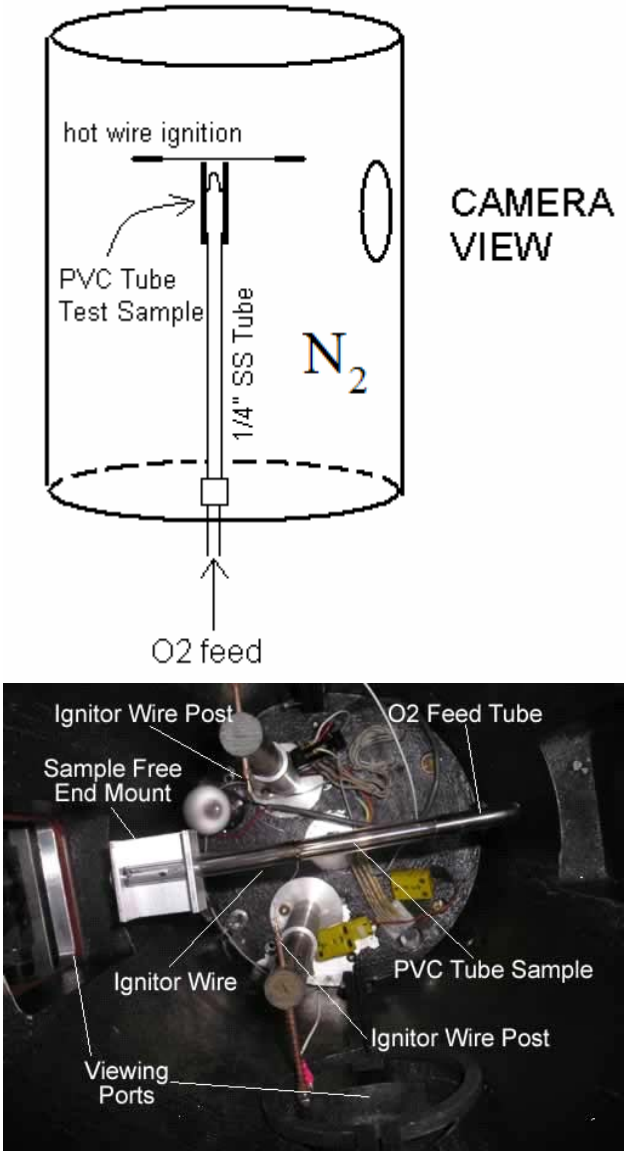

Figure 1: Schematic Diagram (top) of Test Apparatus showing vertical sample, and top view photograph (bottom) showing horizontal sample.

For the vertical tests, a 14.5 cm long ¼" stainless steel tube was attached to the port at the center of the chamber floor. An 18 cm long tube sample was slipped over that tube and held in place at the free end. An ignitor wire (10 cm long 27 gauge Kanthal) was placed in a slit made in the tube sample (sufficiently far from the free end to prevent back diffusion of nitrogen). Flash paper was used in some tests to enhance ignition. For the horizontal tests (the configuration in the photograph of Figure 1), oxygen was delivered through a stainless steel tube formed to provide for horizontal flow.

Two video cameras were mounted on the rig with right angle views. A wide angle view was used primarily to measure the flame spread rate. A closer view was used to observe more detailed flame structure, and only provided useful results for vertical flames. Various camera settings were used in an attempt to improve the quality of the images. A light source on the floor of the chamber was turned on and off at different times to alter the image quality and/or to provide an event signal (such as the start of a drop).

The video was digitized and the flame spread rate was determined using software developed at NASA Glenn [6]. Figure 2 shows the results of a typical tracking in which the position of the leading edge is plotted as a function of time. Zero time and position correspond to the start of the drop. The chamber light was turned off for 0.2 seconds to signal the start of the drop, and the apparent location of the leading edge was affected, explaining the slight reversal in position during the transition period. In retrospect, this signal was unnecessary and it prevented precise analysis of the transition period. An estimate for the characteristic viscous decay time within the tube, $\tau_v = \left(r^2/\nu\right)$, is 0.22 seconds (for inner radius r = 0.18 cm inner radius, and kinematic viscosity, ν = 0.15 cm^2/sec). In all cases, the flame spread rate abruptly changes to a new value within this time frame (even as the flame shape continues to adjust throughout the entire 2.2 seconds of the drop for some cases). The scattered points at the end of the test indicate the rig impacting the air bag and being brought to rest.

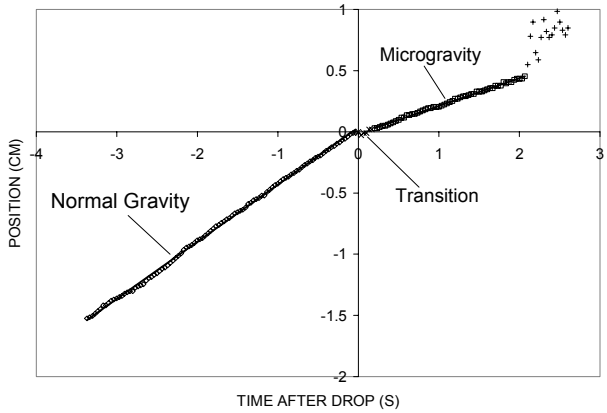

Figure 2: Flame position plotted against time for a typical experiment using tracker software. Test was a horizontal orientation with an opposed flow velocity of 1.61 cm/sec. The slopes from a linear fit are 0.47 cm/sec before the drop and 0.23 cm/sec after the drop.

Fully developed laminar flow is established for all cases. The opposed flow velocity used for all plots is the average flow velocity. The maximum Reynolds number observed is approximately 100.

Results and Discussion

The opposing flow velocity is taken to be the average flow velocity for fully developed laminar flow (flow rate divided by cross-sectional area). Figure 3 shows a comparison of the present results with the corresponding test performed previously in normal gravity for horizontal flame spread. The agreement is excellent, except for the low flow limit of flame spread.

The low flow limit in the present study occurs at an opposing flow velocity of 1.36 cm/s (with a flame spread rate of 0.40cm/s), while the prior study exhibits a limit at a flow velocity of 0.83 cm/s (with a flame spread rate of 0.20 cm/s). Several attempts to ignite flames in normal gravity at a flow velocity of 1.30 cm/s were made using multiple contact points and electrical current pulses through the wire. A flame would establish near the hot wire ignition point, and extinguish as it propagated away. In addition, near the low flow limit, extinction of the weak flame by random fuel vapor bubble microbursts was occasionally observed.

The major differences in the two experiments are the mode of ignition and the external environment. A pilot flame held at the free end was used in the previous study with unlimited time of application. The previous tests were conducted in air in a fume hood, whereas the present test was conducted in a sealed chamber with a nitrogen ambient atmosphere. Due to these experimental differences, the low flow limit in the present study is considered a hot-wire ignition limit, not necessarily a flammability limit. The most significant finding is that a low opposed flow limit exists for this geometry, which is unique in a normal gravity test.

Figure 4 shows the flame spread rates plotted against opposing flow velocity for all tests conducted in the present study. Tests in normal gravity are shown as filled symbols and the corresponding microgravity test in open symbols. Table 1 lists results of power law fits to various segments of these curves. The dotted lines show extrapolations of the fits.

For the microgravity tests, the flame spread rate is independent of orientation. For flow velocities less than 6.3 cm/s, the flame spread rate increases with opposed flow velocity with a power of 1.24. At 6.3 cm/s flow velocity, there is an abrupt change in slope (power law), and the flame spread rate increases with a power of 0.48 for flow velocities between 6.3 and 15.4 cm/s. The power law fit is extrapolated to a flow velocity of 20.4 (shown as a dotted line in Fig. 4), the highest velocity tested. Figure 3 indicates that 20 cm/s is still within the linear low velocity range.

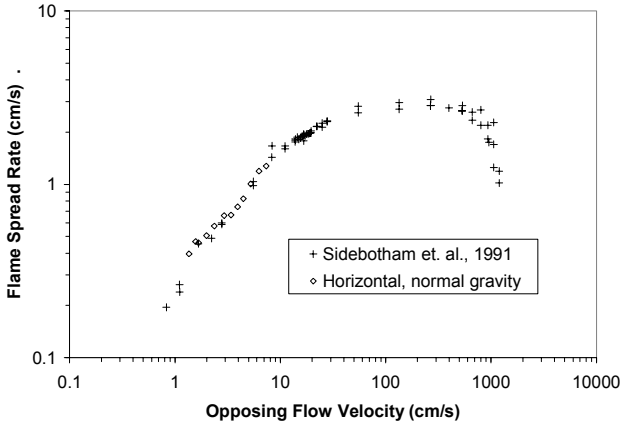

Figure 3: Comparison of previous data obtained in normal gravity and present data during normal gravity portion of the test. Flame spread rate is plotted against opposing flow velocity.

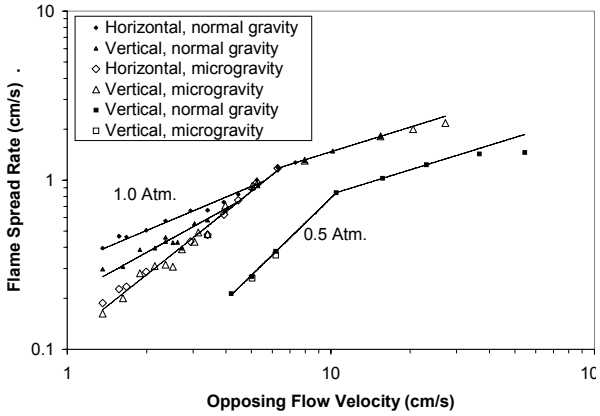

Figure 4: Flame spread rate as a function of opposing flow velocity for all tests conducted for this study. Coefficients of power law fits are listed in Table 1.

Below an opposed flow of approximately 5 cm/s, there is a clear effect of buoyancy. At the low flow limit (1.36 cm/s opposed flow velocity), the horizontal, vertical and microgravity flame spread rates are 0.40, 0.30, and 0.16 cm/s, respectively. The horizontal case has a lower power law exponent (0.65) compared with the vertical case (0.86) which is less than the microgravity case (1.24). The normal gravity curves merge with the microgravity curve at opposed flow velocities of 4.5 cm/s and 5.6 cm/s for vertical and horizontal flames, respectively, with corresponding flame spread rates of 0.75 cm/s and 1.0 cm/s.

There is a strong effect of pressure on flame spread rate. The 0.5 atm curve has generally the same shape as the 1 atm curve but shifted to higher opposed velocities, with a modestly steeper slope in the low range (an exponent of 1.53) and virtually the same slope in the higher range. Most of the shift in the lower pressure curve can be accounted for if the x axis is changed to mass flow rate of oxygen (not shown here), although the lower pressure curve in that case is still slightly offset.

At reduced pressure, there is no effect of gravity for the 2 flow conditions tested. For the test at the lowest flow velocity, a normal gravity flame was established and propagated at a steady rate a distance approximately 1.5 cm at which point it extinguished. Therefore, there is no corresponding microgravity test for this point. The flame spread rate reported in normal gravity is that observed prior to self-extinction. Compared to atmospheric pressure, buoyancy effects at reduced pressure are less apparent because of reduced buoyancy-induced flow and higher opposed flow test conditions.

a) Normal Gravity

b) Microgravity

Figure 5: Photographs of a typical one-sided flame (horizontal orientation) in normal gravity (a) and near the end of the microgravity time (b). Opposing flow velocity is 1.61 cm/s (at atmospheric pressure) and flame spread rates are 0.47 and 0.23 cm/s for normal and microgravity, respectively.

The flame shape varied significantly depending on the flow rate of oxidizer, the orientation and gravity level. The different flame shapes can be classified into 3 different general shapes. The transition from one flame type to another is gradual with increasing opposed flow velocity, and does not appear to correlate with any change in flame spread behavior (for example, with the point of change in slope of the microgravity curve).

Figure 5 shows two photographs from the same horizontal flame test near the low flow limit. Figure 5a shows the flame in normal gravity, just prior to the drop, and Figure 5b shows the flame in microgravity, near the end of the drop period. The flames travel from left to right against an opposed flow velocity of 1.57 cm/s with flame spread rates of 0.47 cm/s and 0.23 cm/s, respectively.

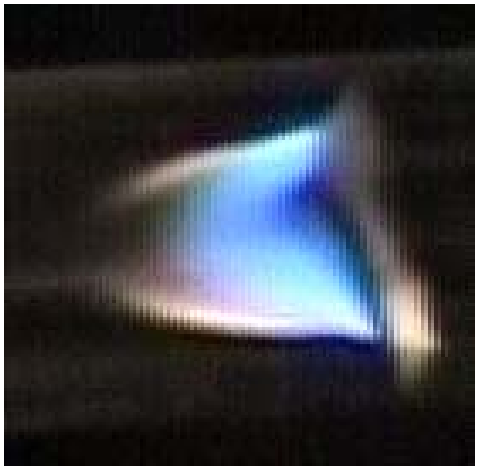

a) Normal Gravity

b) Microgravity

Figure 6: Photographs of a typical two-sided flame (horizontal orientation) in normal gravity (a) and near the end of the microgravity time (b). Opposing flow velocity is 5.4 cm/s (at atmospheric pressure) and flame spread rates are 1.0 and 0.97 cm/s for normal and microgravity, respectively.

The blue flame is not strongly affected by gravity level, but there are subtle differences in the shape of the dark "bubble" around the blue flame. The normal gravity "bubble" is more elongated and streamlined, whereas the microgravity "bubble" is more hemispherical with a thinner tail. The vapor cloud surrounding this "bubble" is believed to be unburned fuel vapor and/or combustion products. The vapor cloud has a distinct leading edge ahead of the blue flame, and interestingly, a distinct trailing edge. The cloud is less uniform in normal gravity, and has a notch in the leading edge near the tube centerline. The normal gravity "bubble" and vapor cloud shapes are attributed to hot buoyant gases pressing against the ceiling and compressing and accelerating the flow between the "bubble" and the hot gases. This may also account for the higher flame spread rate in normal gravity at very low opposed flow velocities.

This spreading flame type does not completely wet the inner surface of the tube and shows a one-sided asymmetry. For horizontal tubes, the leading edge of the flame was always on the bottom of the tube, despite the fact that the ignition points were on the sides of the tube, and the flash paper, when used, was deliberately placed on the upper half of the tube. For vertical tubes, the same asymmetric flame spreading occurred, except the leading edge usually (but not always) ran down at the point of one or the other ignition points where the ignition wire contacted the tube. For the tests reported here, ignition and flame establishment was performed during normal gravity. The results of several tests with ignition during microgravity were inconclusive as to whether there is a fundamental difference in the ignition process in normal and microgravity. It is conceivable that a symmetric flame would establish given unlimited microgravity time, yet no indication of such a shift was apparent. It is equally conceivable that a stable asymmetric flame would exist indefinitely.

This one-sided asymmetric flame shape was observed for opposed flow velocities less than 4.4 cm/s for horizontal flames and 2.7 cm/s for vertical flames (corresponding to flame spread rates of 0.82 and 0.4 cm/s, respectively).

For intermediate opposed flows (Figures 6a and 6b for horizontal normal and microgravity flames, respectively), the flames exhibited a two-sided notched flame where there were two leading edges on opposite sides of the tube. This flame type was found for opposed flow velocities of 5.2 to 6.3 cm/s for horizontal flames, and 3.0 to 4.0 cm/s for vertical flames (corresponding to flame spread rates of 1.00 to 1.19 cm/s and 0.56 to 0.66 cm/s, respectively). In horizontal tubes, the leading edges ran along the top and bottom despite the ignition points of contact being along the sides. During the flame establishment period in normal gravity, the leading edge at the bottom was always forward of the leading edge at the top (Figure 6a). By the end of the microgravity portion of the test, the leading edges were at the same axial position (Figure 6b).

For higher opposed flow rates (Figure 7), the flame leading edge completely wets the inner surface of the tube, and there was no visible difference in flame shape in normal and microgravity, or for vertical or horizontal orientations. As the flow rate increased above a critical flow rate, the inner surface of the tube shows bubbling behind the leading edge. Soot forms on the fuel side of the flame (between the solid and the flame) and the flame resembles inverse diffusion flames, with an oxidizer jet surrounded by fuel.

Figure 7: Photograph of a normal gravity symmetric flame (at 0.5 atm) showing microbubbles in the fuel corresponding with increased heat flux from the strong flame, as indicated by the soot formation. Opposing flow velocity is 11.8 cm/s and the flame spread rate is 1.23 cm/s.

The leading edge of the vapor cloud gives an indication of a preheating length. Figure 8 shows the measured length between the leading edge of the vapor cloud and the leading edge of the blue flame as a function of opposed flow velocity for the horizontal normal and microgravity flames. The preheating length decreases with opposed flow, and is larger for microgravity flames than for normal gravity flames. The preheat length adjusts to its new value within 0.5 sec of microgravity as shown in the inset where the preheat length is plotted against time, with time zero being the start of microgravity. The flame standoff distance, also shown in the inset, is not affected by gravity level and is of the order of 0.5 mm from the fuel surface.

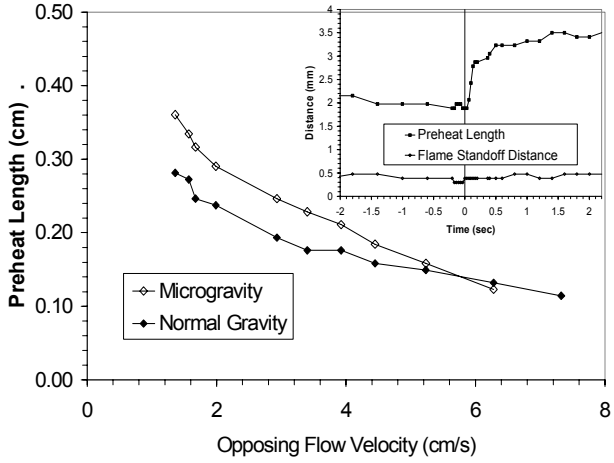

Figure 8: Preheat length (taken to be the distance between the leading edge of the vapor cloud and the leading edge of the blue flame) as a function of opposing flow velocity for horizontal flames in normal and microgravity. The inset shows the preheat length and flame standoff distance as a function of time (with zero time coinciding with the start of the drop) for the test with opposing flow velocity of 1.61 cm/s.

As discussed previously, above ~5 cm/s at 1 atm there is no discernable effect of gravity in the flame shape or flame spread rate. Gravity does not affect the flames at all at 0.5 atm. Since spacecraft ventilation is 5-20 cm/s through the cabin, we suggest that this terrestrial-based test may accurately simulate a material's burning behavior in microgravity in terms of flame spread rate and flame shape. Other related parameters may also be similar, such as heat release rate and combustion product generation rate, although these parameters were not examined here. In this geometry, it is also possible to determine the low opposed flow extinction limits of the material. It may be possible to devise a test method for spacecraft materials screening based upon this geometry.

Conclusions

- A low opposed flow velocity flammability limit exists for this geometry, which is unique in a normal gravity test.
- Buoyancy affects flame spread rate at low flows (<5 cm/s) at atmospheric pressure, and the effects are greater for horizontal flames.
- Buoyancy does not affect flame spread rate at 0.5 atmospheres.
- The flame spread rate adjusts to a step change in gravity level within 0.2 seconds.

Acknowledgements

Work supported by the NASA Faculty Fellowship Program (summer 2003). The contributions of the technical staff of the NASA Glenn 2.2 second drop tower are greatly appreciated. Special thanks to Peter Sunderland for help with all technical aspects of the project, and to Gerald Wolf, MD for introducing this problem to the combustion community.

References

[1] A.C. Fernandez-Pello, S.R. Ray, I. Glassman, 18th Symp. (Int'l) on Comb., The Combustion Institute, 1981, p. 579-587.

[2] S.L. Olson, Combustion Science and Technology, vol. 76 (1991) p. 233-249.

[3] G.W. Sidebotham, G.L. Wolf, Proceedings of the 1989 Technical Meeting of the Eastern States Section of the Combustion Institute.

[4] G.W. Sidebotham, G.L. Wolf, J.B. Stern, R. Aftel in: J.M. Stoltzfus (Ed.), ASTM STP 1111 Flammability and Sensitivity of Materials in Oxygen-Enriched Atmospheres: v5, American Society of Testing and Materials (1991).

[5] G.L. Wolf, G.W. Sidebotham, J.B. Stern, Larygoscope v.104 #7, 1994, p.874-879.

[6] R. Klimek, Wright, T., Spotlight Manual and Software, http://exploration.grc.nasa.gov/spotlight.

TABLE 1: Power Law Fits to Flame Spread Rate Data

$$V_{flame} = AV_{O2}^{n}$$

Gravity Level	***Orientation***	***Pressure***	***Flow Range***	***A***	***n***
Micro	Combined Data	1.0 atm	1.4 – 6.3 cm/s	0.117	1.24
Normal	Vertical	1.0 atm	1.4 - 4.5 cm/s	0.214	0.82
Normal	Horizontal	1.0 atm	1.4 – 5.6 cm/s	0.327	0.62
Micro	Combined Data	1.0 atm	6.3 – 15.4 cm/s	0.484	0.48
Combined	Vertical	0.5 atm	4.2 – 10.5 cm/s	0.023	1.53
Normal	Vertical	0.5 atm	10.5 – 23.0 cm/s	0.273	0.48